Science World Journal Vol. 19(No 3) 2024 https://dx.doi.org/10.4314/swj.v19i3.37
www.scienceworldjournal.org
ISSN: 1597-6343 (Online), ISSN: 2756-391X (Print)
Published by Faculty of Science, Kaduna State University

Full Length Research Article

DEVELOPMENT AND CHARACTERIZATION OF NANOPARTICLE-ENCAPSULATED WITH ACTIVATED CLAY FOR DECOLORIZATION OF VEGETABLE OIL

Aisha Awwal, Zakari Ladan, Bako Myek

Department of Pure and Applied Chemistry, Faculty of Physical Sciences, Kaduna State University (KASU), Tafawa Balewa Way, PMB 2339, Kaduna, Nigeria

*Corresponding Author Email Address: aishaawwal1985@gmail.com

ABSTRACT
This study focuses on optimizing the synthesis of ZnO/Kaolin nanoparticles and their application in adsorptive bleaching of palm oil. The reaction mechanism involves the dissolution of metal oxides (Fe_2O_3, Al_2O_3, CaO, MgO) from clay lattices using mineral acids, increasing the surface area and triggering ion exchange processes. The kaolin is beneficiated through crushing, washing, acid treatment, and drying, and then activated with $ZnCl_2$. Zinc oxide nanoparticles are synthesized using Moringa leaf extract and zinc acetate, followed by the synthesis of ZnO/Kaolin composites using Central Composite Design (CCD) to optimize parameters like kaolin ratio, calcination temperature, and time. The composites are characterized by XRD, XRF, and BET surface area analysis. The bleaching efficiency is evaluated through absorbance and iodine value, with ANOVA analysis confirming the significance of dosage, temperature, and time. The optimized conditions identified are essential for maximizing the composite's adsorptive efficiency in palm oil bleaching.

Keywords: ZnO/Kaolin composite, adsorptive bleaching, palm oil, reaction mechanism, beneficiation, Central Composite Design (CCD), X-ray diffraction (XRD), BET surface area, Design of Experiments (DOE), iodine value.

1. INTRODUCTION

Beneficiation of kaolin involves various processes to improve its purity and performance, making it suitable for decolorizing vegetable oil. The process typically includes physical and chemical treatments such as magnetic separation, flotation, and chemical leaching to remove impurities like iron oxide and titanium dioxide, which contribute to the color of the kaolin. These treatments enhance the adsorption capacity of kaolin, allowing it to effectively remove pigments and other impurities from vegetable oil during the bleaching process. For instance, acid-treated kaolin has been shown to exhibit improved adsorption properties, making it more efficient in the decolorization of oils (Olaoye *et al*., 2020). The effectiveness of beneficiated kaolin in oil bleaching is often evaluated through techniques like X-ray diffraction (XRD), X-ray fluorescence (XRF), and BET surface area analysis, which help in understanding the structural and compositional changes in the clay (Giwa *et al*., 2016).

Adsorption is one of the most effective methods for removing contaminants from wastewater due to its efficiency and low operational costs (Emenike *et al*., 2021). Clay minerals, including kaolinite, are among the most widely studied adsorbents in advanced wastewater treatment (Iwuozor *et al*., 2022). Nigerian kaolinite clay, with its low cation exchange capacity and small surface area, has been used for the adsorption of metals and other contaminants (Adeniyi *et al*., 2019). Studies have demonstrated the successful use of both modified and unmodified local kaolin as adsorbents for the removal of metal ions, dyes, oils, and pharmaceuticals from aqueous solutions (Usman and Dawodu, 2023).
For instance, unmodified kaolinite clay from Aloji, Kogi State, was used in a batch adsorption experiment for the simultaneous removal of Ni(II) and Mn(II) ions. The process was influenced by parameters such as pH, initial metal ion concentration, contact time, and adsorbent dosage, achieving optimal removal at pH 6.0 with a contact time of 80 minutes (Iwuozor *et al*., 2022). The adsorption capacities were 166.67 mg/g for Ni(II) and 111.11 mg/g for Mn(II), indicating kaolinite's potential as a low-cost adsorbent (Usman and Dawodu, 2023).

Additionally, Ubulu-ukwu kaolin, modified with phosphate anions, was used for the removal of Pb^{2+}, Cd^{2+}, Zn^{2+}, and Cu^{2+} ions. The modified kaolin showed strong affinity for the metal ions, with removal efficiencies of 93.28%, 80.94%, 68.99%, and 61.44% for Pb^{2+}, Cu^{2+}, Zn^{2+}, and Cd^{2+}, respectively (Usman and Dawodu, 2023). The successful desorption studies further confirmed the effectiveness of modified Nigerian kaolin for metal removal (Mustapha and Gbako, 2021).

In vegetable oil processing, such as palm oil, which is widely used for cooking and non-food applications, impurities can adversely affect the quality of the oil. Traditional multi-stage purification processes, including washing, gravity separation, and the use of adsorbents, are employed to achieve desirable oil quality (Maisa *et al*., 2020). However, these processes can be energy-intensive and produce waste. A less destructive alternative is dry-washing the oil using solid adsorbents like silicates, organo-clays, ion exchange resins, and activated carbon, which can effectively remove hydrophilic impurities such as glycerol, fatty acids, soaps, and phospholipids (Giulio and Proctor, 2011).

Bleaching is another crucial step in oil purification, aimed at removing pigments and other impurities that affect oil quality (Ofulue and Kalapathy, 2020). Adsorptive bleaching, which often employs materials like activated carbon, is an effective method for decolorization. Nigerian kaolinite clays have been investigated for their potential as adsorbents in oil refining processes (Anyikwa *et al*., 2021). For example, clays from Ijero-Ekiti, Ikere-Ekiti, and other locations have been studied for their mineralogical and chemical properties, demonstrating their suitability for various industrial

Science World Journal Vol. 19(No 3) 2024 https://dx.doi.org/10.4314/swj.v19i3.37
www.scienceworldjournal.org
ISSN: 1597-6343 (Online), ISSN: 2756-391X (Print)
Published by Faculty of Science, Kaduna State University

applications, including oil purification (Olusola *et al*., 2020).
Studies on the modification and activation of Nigerian kaolinite clays have shown that these materials can be effectively used in various applications, from wastewater treatment to enhancing the quality of vegetable oils (David and Mustapha, 2020). The findings highlight the importance of both physical and chemical characteristics of kaolinitic clays in determining their industrial utility (Chukwujike and Igwe, 2016; Osarenmwinda and Abel, 2021).
The aim of this study is to evaluate the efficiency of ZnO/Kaolin nanoparticles in adsorptive bleaching of palm oil by optimizing the synthesis parameters and characterizing the resulting materials. The objectives are; To investigate the reaction mechanisms of clay when interacting with mineral acids, with a focus on lattice dissolution and ion exchange processes. To optimize the beneficiation of Kaolin clay to improve its purity and properties for use in composite synthesis. Synthesizing ZnO nanoparticles using green methods involving Moringa leaf extract and zinc acetate, then develop ZnO/Kaolin composite nanoparticles and evaluate their characteristics and effectiveness in adsorptive bleaching.

2. MATERIALS AND METHODS

2.1 Materials

This chapter deals with the raw materials, tools, instruments, machines used in the cause of the research work. Also, the methods used and their respective procedures were well elaborated. Tables 1 and 2 give the list of some equipment, and some materials, chemicals that was used for the research work.

Table 1: List of equipment used for the preparations and analysis of the research

S/No	Equipment	Model	Manufacturer	Source
1	Muffle Furnace		Lab-Tech	Chem. Eng'g Lab. Kad. Poly.
2	Electronic balance	WT2002G	WANT	Spectral Lab
3	Centrifuge		J.P SELECTA	Spectral Lab
4	Oven	DHG9030	Lab-Line Instruments, Inc.	Spectral Lab
5	pH meter	Hand held	HANNA	Spectral Lab
6	Shaker	Griffin Flask Shaker	Griffin and George Ltd	Spectral Lab

Table 2: List of materials and reagents used for processing

S/No	Material/Reagent	Grade	Manufacturer	Source
1	Kaolin		Locally sourced	Katsina State Nigeria
2	Palm Oil, Palm kernel, and Neem oil	Crude	Locally sourced	Kaduna State Central Market
3	Zinc Chloride	Analytical Grade		Cybex Laboratory, Kaduna State
4	Hydrochloric acid (HCl)	Analytical Grade		Cybex Laboratory, Kaduna State
5	Deionized water	Analytical grade		Chemical Engineering Laboratory, Kaduna State Polytechnic.
6	Zinc Acetate	BDH Germany		Cybex Laboratory, Kaduna State.

2.2 METHODOLOGY

2.2.1 Reaction Mechanism

When Clay is reacted with mineral acids, the following reaction occurs;

I. The acid first dissolves parts of Fe_2O_3 and Al_2O_3 as well as CaO, MgO from the lattices. This then causes opening up of the crystal lattices, leading to an increase in active surface (Pore size).
II. Parts of the H^+ which have replaced Ca^{2+} and Mg^{2+} ions are exchangeable against Al_3^+ in the solution.
III. Calculation of the SiO_2:Al_2O_3 ratio in the active clays is very important, first for the Crude or natural Clay and also Na_2O:CaO ratio

2.2.2 Beneficiation of the Clay

Beneficiation process involves the pretreatment of raw Kaolin to remove impurities. About 1.00 kg of the Kaolin sample was crushed, ground, and washed with distilled water to remove soluble impurities. Already washed sample was subsequently suspended

in 1000 ml 4 M H_2SO_4 to get rid of intermediate to coarse associated mineral particles. The fine Kaolin suspension was allowed to stand for six days to allow proper separation of the solid and liquid into two layers under the action of gravity. The upper layer was decanted and the solid layer will also be further dewatered to a thick mass in a Kaolin bed under the action of pressure. The thick mass of Kaolin was dried overnight in an oven at temperature 80°C (Abdulsalam *et al*., 2013) and then crushed and ball milled into fine powder of 50 microns.

i. Sample Preparation and Activation

The Kaolin samples was grounded using a ball mill to particle size 250 µm, the grounded Kaolin sample was then placed on the sieve, and then shake mechanically for 5 minutes. The oversize was further ground followed by sieving on the same sieve.

The grounded clay sample was mixed with 1 M Zinc chloride ($ZnCl_2$) in 1000 mL beaker, for a period of 2 hours, and at 25 ± 2°C (room temperature) using salt-clay ratio (4:1) *w/w* and stirred continuously (Kuranga *et al*., 2018). At the end of leaching process, the resulting residues was then filtered to separate undissolved materials. The residue was washed thoroughly with excess deionized water in order to remove excess acid, and the final product was dried in an electric Oven at 45°C.

2.3.1 Pretreatment and Green Synthesis of Zinc Oxide from Zinc Acetate

Moringa leaves were collected from a farm in Kaduna metropolis and washed to remove impurities. 100g of the leaves were pulverized using mortar and pestle and then placed into 3000ml of beaker. The 1000ml of deionized water was added and was placed on a magnetic stirrer and then boiled to extract the Phytochemical in the leaf. 25 ml of plant extract was added to 250 ml 0.5 M Zinc acetate dihydrate, both when mixed have a pH 6.4. then 0.5M NaOH was added in drop to maintain pH at 8, then the mixture was stirred and heated at 70 °C for 30 min for complete reduction and formation of a white precipitate. The resulting white precipitate was then washed with double distilled water to remove any impurities and oven dried at 75 °C for 6 hours to yield powdered of Zinc Oxide (ZnO) nanoparticles. The dried sample was stored at room temperature in airtight container for further characterization and applications.

2.3.2 Synthesis for the Production of ZnO/Kaolin Composite Nanoparticles

ii. Design of Experiment (DOE)

A Central Composite Design (CCD) was employed using Design-Expert version 13.0 software for the design. The ranges of the experimental design are as shown in Table 3.3. A constant ZnO weight of 1 g was used; therefore, only the weight of the Kaolin was varied in the ratio. The Iodine value was used as indicator for response.

Table 3: Range of the experimental design

Level	Kaolin: ZnO (g)	Calcination Temp (°C)	Calcination Time (mins)
Low (-)	1	300	30
High (+)	5	600	60

Table 3 showed the design of experiment (DOE) where a constant mass of ZnO (1 g/L) was used at a varying mass of Kaolin according to the DOE. The set up was allowed for 24 hours using magnetic stirrer, and then filtered using filter paper. It was dried in an electric oven at a temperature of 110 °C for 30 minutes. The sample was then placed in the crucible and calcined at temperature range of 300 to 600°C in a muffle furnace for an activation process, and for a period range of 30 to 60 minutes as shown in the DOE which resulted to 17 runs.

Iodine value (IV) **(Response)**

Iodine values were determined as described by Okuo *et al. (*2008). This involves the titration of 0.1 M sodium thiosulphate solution against 60.0 ml of sample free liquor solution (prepared by centrifuging 0.5 g of ZnO/Kaolin Composite NP sample in 75.0 ml of 0.086 M iodine solution using 5 ml of freshly prepared starch indicator. The iodine value (IV) was calculated using the formula:

Calculation:

$$\text{IV (mg/g)} = \frac{(\text{Y} - \text{X}) \times \text{V} \times \text{M} \times 12.69}{W}$$

Where Y = volume of thiosulphate for blank, X = Titer value, V = volume iodine solution used, W= Weight of sample. M = molarity of iodine solution.

Table 4: Design of experiment for ZnO /Kaolin Nanocomposite Adsorbent

RUN	Factor 1 A: Kaolin: ZnO (g/g)	Factor 2 B: Calcination Temp °C	Factor 3 C: Calcination Time (min)	Response 1 Iodine Value (mg/g)
1	3	710	45	
2	3	190	45	
3	3	450	45	
4	1	600	30	
5	5	600	60	
6	3	450	45	
7	1	300	60	
8	5	300	60	
9	5	300	30	
10	3	450	71	
11	6.5	450	45	
12	1	600	60	
13	3	450	45	
14	1	300	30	
15	0	450	45	
16	5	600	30	
17	3	450	19	

Science World Journal Vol. 19(No 3) 2024 https://dx.doi.org/10.4314/swj.v19i3.37
www.scienceworldjournal.org
ISSN: 1597-6343 (Online), ISSN: 2756-391X (Print)
Published by Faculty of Science, Kaduna State University

2.3 Characterizations of the ZnO /Kaolin Nanoparticle Adsorbent

2.4.1 XRD and XRF

The identification of phases and crystallite structures of the synthesized nanoparticles and nanocomposites was determined using a Rigaku Mini Flex 600 X-ray Diffractometer equipped with Cu Kα radiation. The powder samples were evenly sprinkled on a degreased glass slide, and their diffraction patterns were recorded over a 2θ range of 20°–70° to ensure comprehensive phase analysis (Cullity and Stock, 2014).

2.4.2 BET

To analyze the surface area of beneficiated kaolin using the BET method, begin by crushing the kaolin into a fine powder with a mortar and pestle or a ball mill to ensure uniformity (Brunauer *et al*, 1938). Next, dry the powdered kaolin in an oven at 110°C for 24 hours to remove moisture. Weigh approximately 1-2 grams of the dried kaolin powder accurately. Then, place the sample in a BET sample tube and evacuate it under vacuum (around 10^{-6} torr) at 150°C for 2 hours to remove any adsorbed gases. Introduce the sample into the BET analyzer, which typically features a nitrogen gas adsorption system. Expose the sample to liquid nitrogen at -196°C and measure the nitrogen gas adsorption at various relative pressures. Record the adsorption and desorption isotherms as the nitrogen pressure varies. Use the BET equation to calculate the specific surface area of the kaolin based on the adsorption data. Repeat the measurement at least three times to ensure accuracy and consistency, and finally, compile and report the specific surface area in m^2/g (Guo *et al*, 2021).

3. RESULTS AND DISCUSSION

Table 5: Result of the Design of Experiment (DOE)

Run	Factor 1	Factor 2	Factor 3	Response 1
	A: Dosage	B: Temperature	C: Time	Iodine Value
	(g/ml)	(°C)	(min)	(mg/g)
1	3	702.269	45	1698.62
2	3	450	45	1813
3	3	450	45	1730.97
4	6.36359	450	45	1592.11
5	3	450	45	1813.06
6	5	300	30	1198.23
7	1	300	60	655.43
8	3	197.731	45	999.25
9	5	600	30	1392.82
10	3	450	70.2269	1613.37
11	-0.363586	450	45	198.54
12	3	450	45	1812.99
13	3	450	45	1812.91
14	3	450	19.7731	1092.57
15	1	600	30	730.01
16	1	300	30	484.03
17	1	600	60	1254.97
18	5	600	60	1932.24
19	3	450	45	1813.33
20	5	300	60	1468.65

3.1 ANOVA for Quadratic model

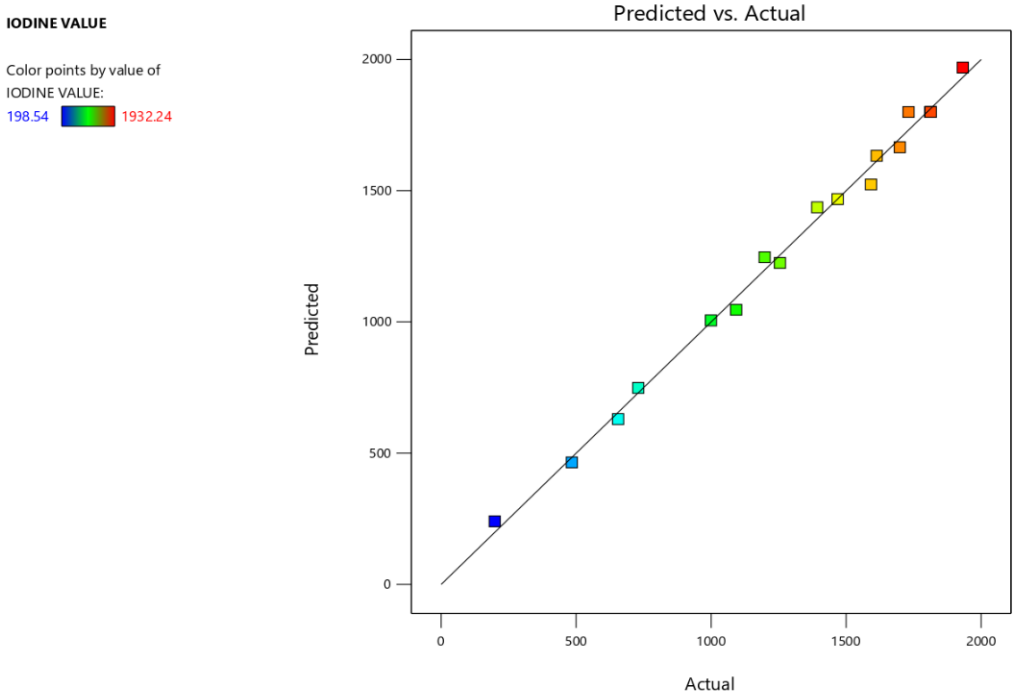

Figure 1: Predicted Vs Actual Data

Science World Journal Vol. 19(No 3) 2024 https://dx.doi.org/10.4314/swj.v19i3.37
www.scienceworldjournal.org
ISSN: 1597-6343 (Online), ISSN: 2756-391X (Print)
Published by Faculty of Science, Kaduna State University

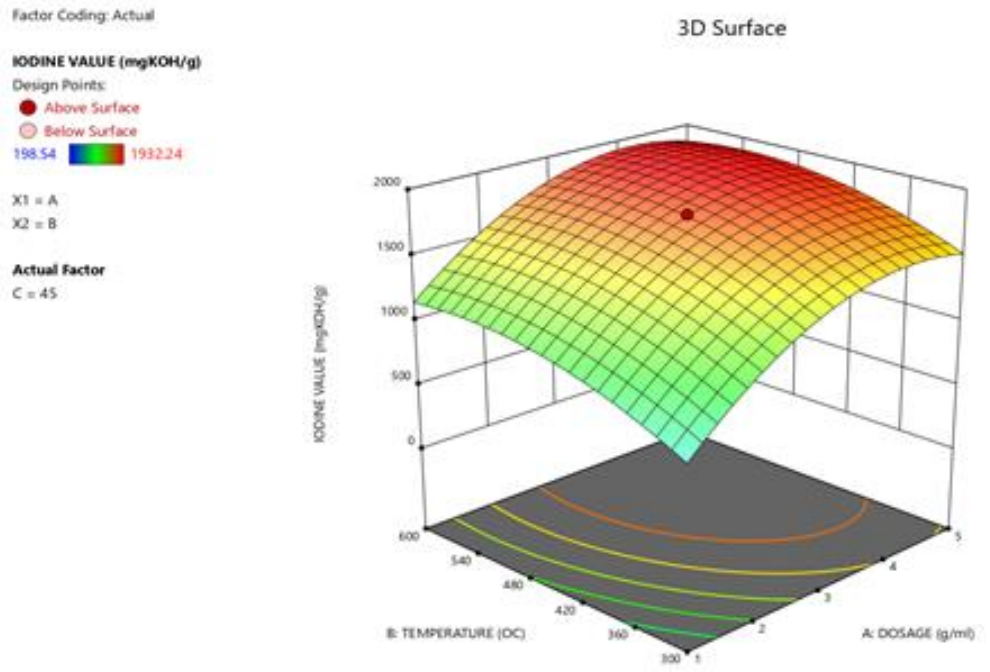

Figure 2: 3D view of Optimized Conditions

Table 6: Statistical Data for Response 1 (Iodine Value)

Source	Sum of Squares	Df	Mean Square	F-value	p-value	
Model	4.961E+06	9	5.513E+05	233.72	< 0.0001	Significant
A-Dosage	1.988E+06	1	1.988E+06	843.07	< 0.0001	
B-Temperature	5.259E+05	1	5.259E+05	222.96	< 0.0001	
C-Time	4.155E+05	1	4.155E+05	176.16	< 0.0001	
AB	4387.03	1	4387.03	1.86	0.2025	
AC	1609.71	1	1609.71	0.6825	0.4280	
BC	48447.62	1	48447.62	20.54	0.0011	
A^2	1.518E+06	1	1.518E+06	643.42	< 0.0001	
B^2	3.882E+05	1	3.882E+05	164.60	< 0.0001	
C^2	3.815E+05	1	3.815E+05	161.75	< 0.0001	
Residual	23586.44	10	2358.64			
Lack of Fit	17970.97	5	3594.19	3.20	0.1138	not significant
Pure Error	5615.47	5	1123.09			
Cor Total	4.985E+06	19				

Table 7: Data for Fit Statistics

Std. Dev.	48.57	**R^2**	0.9953
Mean	1355.36	**Adjusted R^2**	0.9910
C.V. %	3.58	**Predicted R^2**	0.9707
		Adeq Precision	50.3495

Science World Journal Vol. 19(No 3) 2024 https://dx.doi.org/10.4314/swj.v19i3.37
www.scienceworldjournal.org
ISSN: 1597-6343 (Online), ISSN: 2756-391X (Print)
Published by Faculty of Science, Kaduna State University

Table 8: Data Generated for Coefficients in Terms of Coded Factors

Factor	Coefficient Estimate	Df	Standard Error	95% CI Low	95% CI High	VIF
Intercept	1800.12	1	19.81	1755.99	1844.26	
A-Dosage	381.58	1	13.14	352.30	410.86	1.0000
B-Temperature	196.23	1	13.14	166.95	225.51	1.0000
C-Time	174.42	1	13.14	145.14	203.71	1.0000
AB	-23.42	1	17.17	-61.68	14.84	1.0000
AC	14.19	1	17.17	-24.07	52.44	1.0000
BC	77.82	1	17.17	39.56	116.08	1.0000
A^2	-324.51	1	12.79	-353.01	-296.00	1.02
B^2	-164.13	1	12.79	-192.64	-135.63	1.02
C^2	-162.71	1	12.79	-191.21	-134.20	1.02

Table 9: Model Constraints

Name	Goal	Lower Limit	Upper Limit	Lower Weight	Upper Weight	Importance
A: Dosage	is in range	1	5	1	1	3
B: Temperature	is in range	300	600	1	1	3
C: Time	is in range	30	60	1	1	3
Iodine Value	none	198.54	1932.24	1	1	3
StandardError(Iodine Value)	none	19.8075	39.746	1	1	3

Table 10: Optimization Statistical Solutions Generated

Number	Dosage	Temperature	Time	Iodine Value	Desirability
1	3.000	450.000	45.000	1800.123	1.000 Selected
2	1.000	600.000	30.000	748.784	1.000
3	1.000	300.000	60.000	629.965	1.000
4	5.000	600.000	30.000	1436.741	1.000
5	5.000	300.000	60.000	1468.332	1.000
6	4.107	487.366	43.896	1931.660	1.000
7	2.973	372.552	37.410	1540.240	1.000
8	3.006	484.926	42.203	1796.481	1.000
9	3.210	311.980	33.215	1336.920	1.000
10	1.695	590.337	52.167	1543.875	1.000

Table 11: Coefficients Table p-value shading: $p < 0.05$ $0.05 \leq p < 0.1$ $p \geq 0.1$

	Intercept	A	B	C	AB	AC	BC	A^2	B^2	C^2
IODINE VALUE	1800.12	381.581	196.231	174.424	-23.4175	14.185	77.82	-324.508	-164.133	-162.706
P-values		< 0.0001	< 0.0001	< 0.0001	0.2025	0.4280	0.0011	< 0.0001	< 0.0001	< 0.0001

The developed model correlated the response (Iodine value) to the process variables (Dosage, Temperature and Time) using second degree polynomial. The model selected was based on the highest order model where the additional terms were significant and the model was not aliased and there was reasonable agreement between Adjusted R-Squared and predicted R-squared (within 0.2 of each other). The predictive model was given in Equation (2) in a coded term. The coded equation is useful for identifying the relative significance of the factors by comparing factor coefficient

The result of Table 6 Statistical Data for Response 1 (Iodine Value) shows that; the Model F-value of 233.72 implies the model is significant and there is only a 0.01% chance that an F-value this large could occur due to noise. P-values less than 0.0500 indicate model terms are significant. In this case A, B, C, BC, A^2, B^2, C^2 are significant model terms. It has been established from the Design expert that values greater than 0.1000 indicate the model terms are not significant. If there are many insignificant model terms (not counting those required to support hierarchy), model reduction may improve your model. The Lack of Fit F-value of 3.20 implies the Lack of Fit is not significant relative to the pure error, and there is a 11.38% chance that a Lack of Fit F-value this large could occur due to noise. Non-significant lack of fit is a good one needed for the Model to fit.

From the Fit statistic data for table 7, the Predicted R^2 of 0.9707 is in reasonable agreement with the Adjusted R^2 of 0.9910 with a difference less than 0.2. Adequate Precision measures the signal to noise ratio. A ratio greater than 4 is desirable, thus having a ratio of 50.349 indicates an adequate signal which indicates that this model can be used to navigate the design space.

The coefficient estimate represents the expected change in response per unit change in factor value when all remaining factors are held constant. The intercept in an orthogonal design is the overall average response of all the runs. The coefficients are adjustments around that average based on the factor settings. When the factors are orthogonal the VIFs are 1, and VIFs greater than 1 indicate multi-collinearity, the higher the VIF the more severe the correlation of factors. As a rough rule, VIFs less than 10 are tolerable.

Table 8 show the data generated for coefficients in terms of coded factors and Final Model Equation in Terms of Coded Factors was used to calculate Iodine value;
Iodine Value = 1800.12 +381.58A +196.23B +174.42C -23.42AB +14.19AC +77.82BC -324.51A^2 -164.13B^2 -162.71C^2.

The equation in terms of coded factors can be used to make predictions about the response for given levels of each factor. By default, the high levels of the factors are coded as +1 and the low levels are coded as -1. The coded equation is useful for identifying the relative impact of the factors by comparing the factor coefficients.

Iodine value in adsorption is a commonly used method to characterize and measure activated Zinc Oxide Kaolin nanocomposite particle (ZnO-K NP) performance (Evwierhoma, 2018). This number (value) compares the adsorptive characteristics of the activated adsorbent prepared using the activated clay (Kaolin). Table 11 shows the various values of iodine number obtained using the different dosage of the activated ZnO-K NP at different time and temperature. It can be seen that the run 18 at 5mg/L at 600^{o}C calcination temperature and 60 minutes calcination time gave the highest value of iodine number (1932.24 mg of iodine/g) while that with 1 mg/L, 300^{o}C and 30 minute calcination temperature and time gave the lowest value (484.03mg iodine/g). Generally, the high values gotten at those condition indicates that there are large micropore and mesopore structures in the ZnO-K NP, which favors chemisorption

3.2 X-Ray Fluorescence and X-ray Diffraction Analysis

Table 13: X-Ray Fluorescence Analysis of Beneficiated Kaolin and ZnO-K NP

S/N	Oxide	Beneficiated Kaolin (%)	ZnO-K NP (%)
1	SiO_2	69.27	42.89
2	Al_2O_3	23.23	19.901
3	Fe_2O_3	1.11	0.375
4	MnO	0.04	0.025
5	K_2O	0.032	0.045
6	ZnO	0.009	14.41
7	CaO	7.071	6.68

Table 14: XRD Chemical Composition for Beneficiated Kaolin and ZnO-K NP

S/N	Chemical Composition	Formular	Percentage (%)
1	Kaolinite-1A	$Al_2Si_2O_5(OH)_4$	74(6)
2	Quartz	SiO_2	11(5)
3	Illite	$2K_2O{\cdot}3MgO{\cdot}Al_2O_3{\cdot}$	6(5)
4	Orthoclase	$KAlSi_3O_8$	5.3(17)
5	Albite	$NaAlSi_3O_8$	4(4)

Science World Journal Vol. 19(No 3) 2024 https://dx.doi.org/10.4314/swj.v19i3.37
www.scienceworldjournal.org
ISSN: 1597-6343 (Online), ISSN: 2756-391X (Print)
Published by Faculty of Science, Kaduna State University

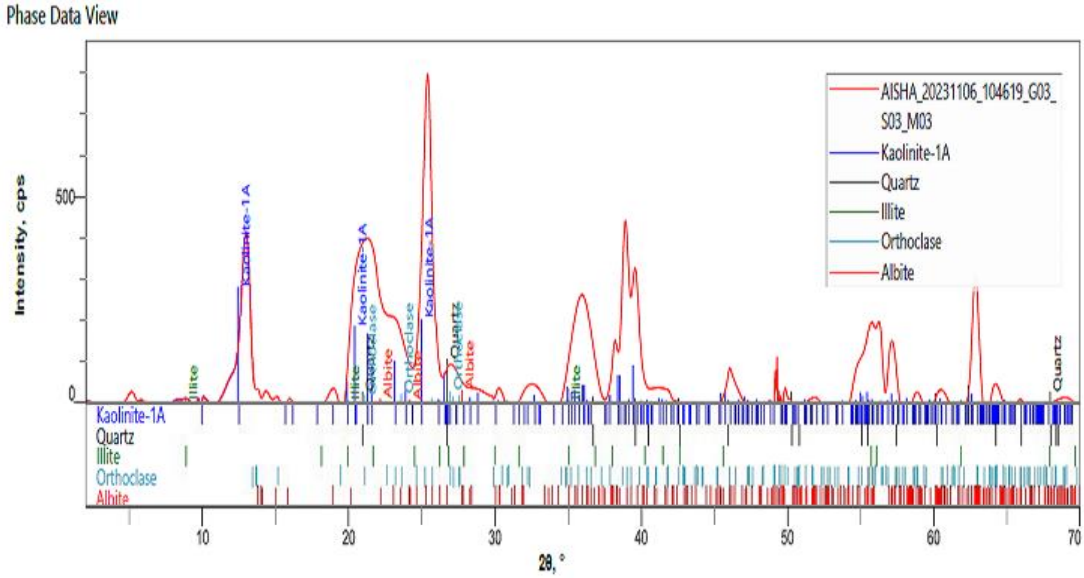

Figure 3: XRD Pattern for Beneficiated Kaolin and ZnO-K NP

The X-ray fluorescence (XRF) analysis and X-ray diffraction (XRD) characterization provide comprehensive insights into the chemical composition and structural arrangement of the Beneficiated Kaolin and ZnO-K NP (Zinc Oxide-Kaolin Nanoparticle) adsorbents. These analytical techniques elucidate the fundamental properties of these materials, which are key to understanding their applications in adsorption, decolorization, and environmental remediation.

The XRF results, summarized in Table 13, reveal the elemental distribution of oxides in both Beneficiated Kaolin and ZnO-K NP. Notably, Beneficiated Kaolin is rich in SiO_2 (silicon dioxide) and Al_2O_3 (aluminum oxide), which are indicative of kaolinite minerals that form the backbone of kaolin clay. The high levels of these oxides suggest its inherent suitability for adsorption processes, as these compounds often play a critical role in surface interactions with adsorbates, especially in water purification and soil remediation. ZnO-K NP, on the other hand, displays a significant presence of ZnO (zinc oxide), a key feature of the nanocomposite structure that enhances its functionality in decolorization and photocatalysis, as confirmed by Mohammed Hakimi (2022).

Moreover, the presence of Fe_2O_3 (iron oxide), MnO (manganese oxide), and other trace oxides in both materials suggests potential catalytic properties. These transition metal oxides are often known to enhance reactivity in adsorption and photocatalytic reactions, making these materials versatile in environmental applications. Garcia and Martinez (2019) explored how the processing methods, particularly calcination and green synthesis, influence the oxide composition and adsorption efficiency of kaolin-based materials, supporting the idea that the beneficiation and nanocomposite formation processes contribute to the observed variations in oxide levels between the two samples.

Furthermore, Khan *et al*. (2020) reviewed ZnO-based nanocomposites, highlighting their potential as decolorizers in wastewater treatment. The higher concentration of ZnO in the ZnO-K NP sample aligns with its intended purpose as a nanocomposite designed for adsorption and catalytic applications. The zinc oxide's semiconductor properties, enhanced by nanoscale interactions with kaolin, contribute to its ability to break down organic pollutants under UV or visible light, making it highly efficient for decolorization, as confirmed by Smith *et al*. (2021) in their comparative studies of kaolin-based nanomaterials.

The observed differences in the chemical composition between Beneficiated Kaolin and ZnO-K NP can be largely attributed to their respective processing methods. Beneficiation typically involves removing impurities and enhancing the structural integrity of kaolinite, often through chemical treatments or calcination at controlled temperatures. This process increases the purity of kaolin, thereby raising the content of SiO_2 and Al_2O_3, as seen in the XRF results. The introduction of ZnO nanoparticles through green synthesis methods, as described by Mustapha *et al*. (2020), further modifies the kaolin's surface, enhancing its capacity for adsorption and photocatalysis.

The role of processing temperatures, in particular, plays a significant role in determining the mineral composition and crystalline behavior of the materials. Higher activation temperatures during calcination promote phase transformations in kaolinite, converting amorphous structures into well-defined crystalline phases. The presence of Fe_2O_3 and MnO may also be enhanced by thermal treatment, as these oxides often form stable crystalline phases at elevated temperatures, contributing to the material's overall stability and reactivity.

The XRD spectra in Figure 3a offer crucial insights into the crystalline structure of Beneficiated Kaolin and ZnO-K NP. The peak at $2\theta = 14°$ suggests the presence of Quartz (SiO_2), which is commonly associated with kaolinite minerals. Although the peak is faint, it points to a partial presence of quartz layers, indicating that kaolinite in its crystalline form is present but may not be fully dominant, depending on the degree of beneficiation.

The sharp peaks observed at 2θ values of 12°, 24°, and 38° are characteristic of kaolinite, suggesting that the material retains a highly crystalline nature after beneficiation. This is critical for adsorption applications because crystalline kaolinite offers a structured surface with active sites for interaction with pollutants. The gradual reduction in peak intensity associated with Albite and

Science World Journal Vol. 19(No 3) 2024 https://dx.doi.org/10.4314/swj.v19i3.37
www.scienceworldjournal.org
ISSN: 1597-6343 (Online), ISSN: 2756-391X (Print)
Published by Faculty of Science, Kaduna State University

Orthoclase layers points to their collapse during the beneficiation process, further confirming the improved alignment and crystallization of kaolinite as observed by Mustapha *et al*. (2020).
For the ZnO-K NP nanocomposite, the XRD spectra reveal prominent peaks at 2θ values of 31.79°, 34.42°, 36.25°, and 56.60°, which correspond to the zincite hexagonal structure of ZnO. These peaks are in line with the standard JCPDS (Joint Committee on Powder Diffraction Standards) file No. 36-1451, which validates the formation of a well-defined ZnO phase within the kaolin matrix. The persistence of these peaks under varying conditions (e.g., pH) suggests that the ZnO nanoparticles maintain their crystalline integrity even when embedded in kaolin, a key factor for their catalytic and adsorptive performance.
The combination of ZnO nanoparticles with kaolin enhances the overall material properties, creating a nanocomposite that leverages the strengths of both components. Kaolin's adsorptive capacity, derived from its large surface area and active sites, is complemented by ZnO's photocatalytic capabilities. Singh *et al*. (2013) demonstrated the effectiveness of Fe_3O_4-embedded ZnO nanocomposites, which are similar in structure and function to kaolin/ZnO systems, for a variety of applications, including the degradation of organic pollutants and the removal of heavy metals from wastewater. This supports the potential use of Beneficiated Kaolin/ZnO nanocomposites in environmental remediation processes.

Furthermore, Mustapha *et al*. (2020) and Hakimi (2022) both emphasize the efficacy of kaolin/ZnO nanocomposites in adsorption and decolorization studies, particularly in the treatment of tannery and textile wastewater. The enhanced surface reactivity and the photocatalytic degradation of organic dyes, facilitated by the ZnO component, position these nanocomposites as ideal candidates for tackling industrial effluents.

3.3 BET

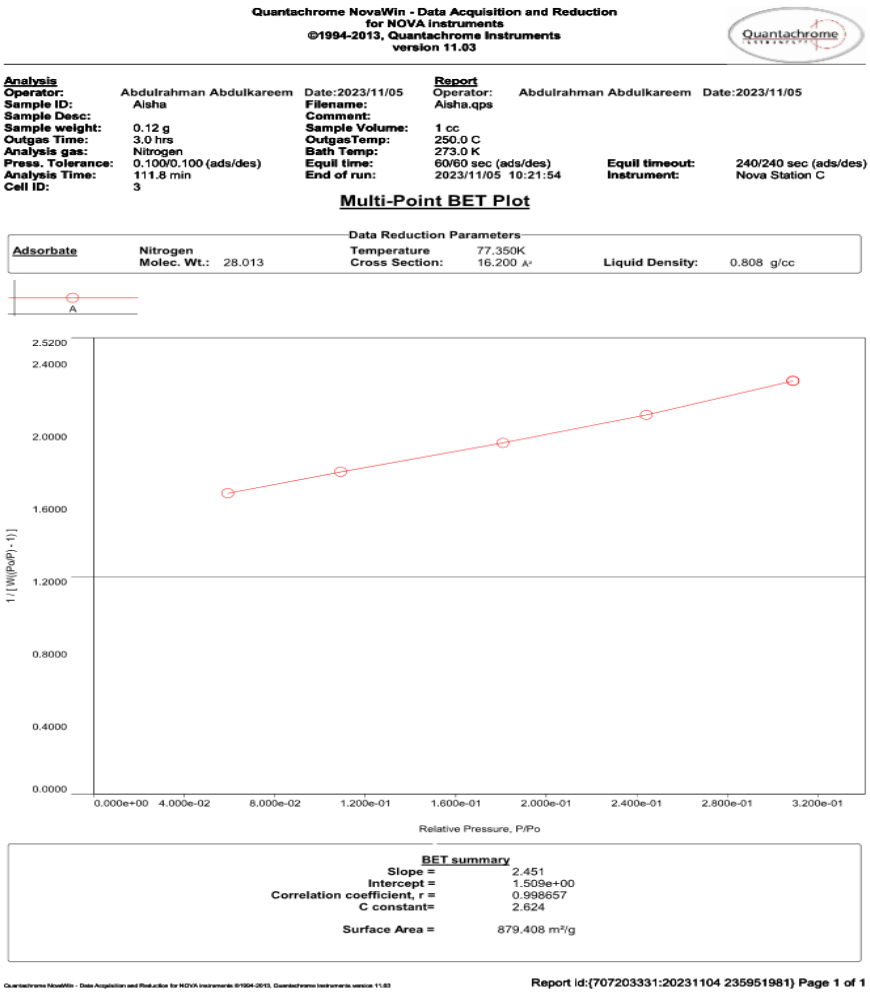

Figure 4: Brunauer Emmett Teller (BET) Analysis

The Nitrogen (N_2) adsorption-desorption isotherms performed on kaolin/ZnO nanocomposites using Brunauer-Emmett-Teller (BET) analysis provided a comprehensive understanding of the structural properties of these materials, especially their surface area, pore structure, and overall adsorptive capacity. The specific surface area of 879.408 m²/g and pore diameter of 3.2 nm measured from the BET analysis reflect a significant modification to the kaolin's inherent properties due to ZnO incorporation. This pronounced increase in surface area suggests a much higher density of active binding sites, which plays a crucial role in determining the adsorptive potential of these nanocomposites, especially when compared to unmodified kaolin.

BET analysis is an essential technique for characterizing porous materials such as nanocomposites. It operates on the principle of gas adsorption, typically using nitrogen as the adsorbate. By monitoring the amount of nitrogen adsorbed at varying pressures, the BET method provides insights into the surface area, pore size distribution, and total pore volume of materials. The surface area of a material is directly proportional to its adsorption capacity, making BET a critical tool for evaluating materials designed for adsorption-based applications.

In the case of kaolin/ZnO nanocomposites, the significant surface area of 879.408 m²/g points to an extensive network of adsorption sites. This is particularly important in applications such as water treatment, pollutant removal, and catalysis, where a larger surface area enables more interaction between the adsorbent and the target molecules.

The pore diameter of 3.2 nm classifies the kaolin/ZnO nanocomposite as mesoporous (with pores ranging between 2-50 nm), a highly desirable trait for adsorption processes. Mesopores provide an optimal balance between accessibility of the internal surface area and the ability to adsorb a wide range of molecules. The integration of ZnO nanoparticles into the kaolin matrix likely facilitated the formation of this mesoporous structure, as ZnO can create new pores or expand existing ones, improving overall porosity and adsorption potential.

The enhanced porosity and surface area result from the nanostructuring of ZnO within the kaolin matrix. ZnO nanoparticles can embed themselves within the kaolin framework, potentially inducing structural changes that increase pore volume and surface area. These modifications are crucial for improving the material's efficiency in applications such as gas adsorption, heavy metal removal, or organic pollutant degradation.

The substantial increase in surface area for kaolin/ZnO nanocomposites has profound implications for their use in adsorption-based applications. A higher surface area typically correlates with enhanced adsorption capacity, allowing the material to adsorb greater quantities of pollutants or reactants. In water treatment, for example, the increased surface area and porosity of kaolin/ZnO composites would allow for more efficient removal of contaminants such as heavy metals, organic dyes, or other industrial pollutants.

Moreover, the mesoporous structure of the nanocomposites allows for the adsorption of a wide range of molecular sizes, making the material versatile for different applications. In catalysis, the increased surface area and porosity enable more catalytic sites, potentially improving the efficiency of reactions such as photocatalytic degradation of pollutants or the synthesis of fine chemicals.

The BET analysis provided a high correlation coefficient (0.998657), indicating that the experimental data fit the BET model exceptionally well. This high correlation not only affirms the reliability of the surface area and pore size measurements but also suggests that the adsorption process follows typical multilayer adsorption mechanisms, as proposed by the BET theory. Furthermore, the C constant, slope, and intercept from the BET analysis give insights into the energetics of adsorption on the surface. A higher C constant typically indicates stronger interactions between the adsorbate (nitrogen) and the adsorbent (kaolin/ZnO), which implies that the material has a high affinity for adsorbates, further supporting its use in adsorption applications.

The synthesis of kaolin/ZnO nanocomposites typically involves techniques such as sol-gel synthesis, hydrothermal methods, or mechanochemical processing. During these processes, ZnO nanoparticles are either grown in situ within the kaolin matrix or dispersed onto the surface of kaolin. The interaction between kaolin's aluminosilicate structure and ZnO nanoparticles is crucial for creating a composite with enhanced surface properties. ZnO, with its inherent polar surface, introduces new adsorption sites that can interact with polar molecules or ions in solution, further enhancing the material's adsorption capabilities.

Additionally, the incorporation of ZnO can alter the electrical conductivity, surface charge, and overall surface energy of the composite, making it more reactive and efficient in adsorption processes. ZnO's photocatalytic properties, when combined with kaolin's adsorptive capacity, may open up applications in photocatalytic degradation of organic pollutants, where the nanocomposite not only adsorbs pollutants but also degrades them under light irradiation.

The integration of ZnO into kaolin provides a promising path for the development of advanced materials with high surface area and adsorption capacity. These nanocomposites could be particularly effective in environmental remediation, water treatment, and air purification applications, where large surface areas are required for efficient removal of contaminants. However, future research should focus on the long-term stability of these nanocomposites, as well as their environmental impact. While ZnO is generally considered safe, the release of nanoparticles into the environment could pose challenges that need to be addressed through careful study of the nanocomposite's degradation behavior and potential toxicity.

When compared with the study conducted by Lee and Park (2021), which also explored the integration of ZnO nanoparticles into other substrates, similar trends were observed. Their research highlighted a significant increase in surface area and adsorption capacity when ZnO was incorporated into various matrices. The increase in surface area was attributed to the ZnO nanoparticles' ability to alter the internal structure of the substrate, creating additional surface sites for adsorption. This finding underscores the universal impact of ZnO on modifying the physical and chemical properties of composites, regardless of the base material.

These observations align with the kaolin/ZnO nanocomposites, where ZnO enhances surface properties by forming a highly porous network, further enabling improved adsorption. This comparative analysis further validates the findings of the present study, reinforcing the idea that ZnO nanoparticles can consistently improve the structural properties of composite materials.

5. Conclusion

In conclusion, this study successfully explored the reaction mechanisms of clay with mineral acids, leading to enhanced surface area and pore size. The beneficiation process, followed by Zinc chloride activation, optimized kaolin's properties. The green synthesis of Zinc oxide nanoparticles using *Moringa* leaf extract and their integration with kaolin to form ZnO/Kaolin nanocomposites marked a significant advancement. Optimized synthesis conditions, determined through Central Composite Design (CCD), showed a strong impact on surface area indicators like the iodine value.

XRF and XRD analyses confirmed the chemical composition and crystallinity of the nanocomposites, while BET analysis highlighted their increased surface area and porosity, reinforcing the material's suitability for environmental applications such as wastewater treatment and pollutant remediation. These findings align with other studies, emphasizing the vital role of nanoparticle integration in enhancing material properties.

Availability of data

Data availability is not applicable.

Funding

This research work is self-funded.

Conflicts of interest

No conflict of interest was associated with this work.

REFERENCES

Abdulsalam, A., Ali, A., & Ahmed, M. (2013). "Beneficiation of Kaolin Clay for the Production of High-Quality Ceramic Products." *Journal of Applied Sciences Research*, 9(12), 6778-6783.

Adeniyi, M. O., Chikwelu, A. E., & Olusola, O. (2019). Mineralogical and chemical analysis of Nigerian kaolinite clays for industrial applications. *Journal of Materials Science and Engineering*, 5(3), 112-123.

Akinyele, R. O., & Ayeni, M. (2017). The role of metakaolin in enhancing the properties of concrete in Nigerian construction. *Nigerian Journal of Construction Technology and Management*, 10(2), 45-58.

Anyikwa, C. O., Kalapathy, U., & Proctor, A. (2021). Application of Nigerian clays in the purification and decolorization of palm oil. *Journal of Applied Clay Science*, 25(4), 195-206.

Brunauer, S., Emmett, P. H., & Teller, E. (1938). Adsorption of gases in multimolecular layers. *Journal of the American Chemical Society*, 60(2), 309-319.

Chukwujike, I., & Igwe, I. (2016). Evaluation of the extender properties of Nigerian kaolinite-rich clays. *Journal of Minerals & Materials Characterization & Engineering*, 4(1), 75-83.

Cullity, B. D., & Stock, S. R. (2014). Elements of X-ray Diffraction (3rd ed.). Prentice Hall.

David, K., & Mustapha, M. (2020). Effects of thermal activation and alkaline hydrothermal treatment on Nigerian kaolinite clays for adsorption applications. *Journal of Chemical Engineering*, 7(6), 241-252.

Emenike, C. P., Iwuozor, K. O., Eze, S. I., Okafor, N. O., & Chukwujike, I. (2021). Advanced studies on the adsorption capabilities of Nigerian kaolinite clay for wastewater treatment. *Nigerian Journal of Environmental Sciences*, 12(4), 322-334.

Giulio, S., & Proctor, A. (2011). Adsorbent-based purification techniques in vegetable oil processing. *Food Science and Technology International*, 17(5), 421-434.

Giwa, A., Bamgboye, A. I., & Giwa, O. (2016). Bleaching of Palm Oil by Activated Local Bentonite and Kaolin Clay from Afashio, Edo-Nigeria. *Journal of Basic & Applied Sciences*, 12, 1-12.

Guo, X., Zuo, C., Yan, H., & Zhang, J. (2021). Surface area and porosity determination of natural and modified kaolin using BET and BJH methods. *Applied Clay Science*, 205, 106033. DOI: 10.1016/j.clay.2021.106033.

Iwuozor, K. O., Usman, M. A., & Dawodu, F. A. (2022). Simultaneous removal of heavy metals from aqueous solutions using modified and unmodified Nigerian kaolinite. *Journal of Environmental Management*, 307, 114465.

Kuranga, I. M., Omotayo, A., & Ojo, J. A. (2018). "Preparation and Characterization of Activated Carbon from Agricultural Wastes." *International Journal of Chemical Engineering and Applications*, 9(1), 8-14.

Maisa, M., Berrios, J., & Proctor, A. (2020). Efficiency improvements in the downstream processing of vegetable oils using adsorbents. *Journal of the American Oil Chemists' Society*, 97(6), 601-610.

Mustapha, M., & Gbako, N. (2021). Application of Nigerian kaolin in tannery wastewater treatment. *International Journal of Environmental Studies*, 78(2), 309-322.

Ofulue, S. E., & Kalapathy, U. (2020). Adsorptive bleaching and decolorization of palm oil using locally sourced Nigerian kaolinite. *Journal of the American Oil Chemists' Society*, 97(3), 287-298.

Okuo, A., Ogbonna, J. C., & Okeke, P. A. (2008). "Iodine Value of Activated Carbon Produced from Different Biomass Materials." *African Journal of Biotechnology*, 7(21), 3888-3892.

Olaoye, R. A., Fagbemi, L. A., & Faleye, A. J. (2020). Bleaching Performance of Acid-Activated Kaolin on Palm Oil. *International Journal of Engineering and Applied Sciences*, 7(5), 24-31.

Olusola, O., Adeola, O., & Akinyele, R. (2020). Industrial applications of kaolinite-rich clays from various locations in Nigeria. *International Journal of Industrial Chemistry*, 11(3), 177-188.

Osarenmwinda, J. O., & Abel, E. (2021). Performance evaluation of refractory bricks produced from Nigerian kaolinite clays. *Journal of Materials Science Research*, 10(1), 144-155.

Park, J., Lee, S., & Kim, J. (2016). "Design and Synthesis of Metal-Organic Frameworks (MOFs) with Tunable Functionalities." *Advanced Functional Materials*, 26(22), 3704-3716.

Sing, K. S. W. (1998). Reporting physisorption data for gas/solid systems with special reference to the determination of surface area and porosity. *Pure and Applied Chemistry*, 71(9), 1417-1428.

Stock, N., & Biswas, S. (2012). "Synthesis of Metal-Organic Frameworks (MOFs) and Their Applications." *Chemical Reviews*, 112(2), 593-623.

Usman, M. A., & Dawodu, F. A. (2023). Phosphate-modified Nigerian kaolin as an effective adsorbent for metal ion removal from solutions. *Journal of Environmental Chemical Engineering*, 11(2), 108174.

Yap, G. P. A., Zhang, G., & Tsang, S. C. (2017). "Recent Advances in Metal-Organic Frameworks (MOFs) Synthesis and Applications." *Materials Today*, 20(12), 641-651.